Back grating optimization for light trapping in thin-film quantum dot solar cells

Back grating optimization for light trapping in thin-film quantum dot solar cells

F. Elsehrawy[(1)], F. Cappelluti[(1)], T. Aho[(2)], T. Niemi[(2)], V. Polojärvi[(2)], M. Guina[(2)]*

(1) Department of Electronics and Telecommunications, Politecnico di Torino, Torino, 10129, Italy

(2) Optoelectronics Research Centre, Tampere University of Technology, P.O. Box 692, FI-33101 Tampere, Finland

*federica.cappelluti@polito.it

Keywords: light-trapping, diffraction grating, quantum dot, thin-film, solar cell

Abstract

The work presents the design of a diffraction back grating for light-trapping in thin-film GaAs-based quantum dot solar cells. Uni-periodic and bi-periodic gratings made of off-the-shelf almost transparent dielectric materials routinely used in photolithography are considered. Gratings are wave-optics simulated by rigorous coupled wave analysis. Optimizing the shape and geometrical aspect ratio of the grating, almost quadrupled photocurrent from quantum dots is demonstrated.

1. Introduction

The demand for high efficiency solar cells requires the development of innovative concepts. One promising approach is increasing the cell optical path length through light-trapping [1]. This allows thinning the photovoltaic active region while keeping the short circuit current constant and reducing volume recombination loss, thus achieving higher open circuit voltage and efficiency. Cell thinning is also advantageous in terms of light weight and cost. In fact, light-trapping approaches are extensively investigated in several photovoltaic technologies [1]-[3], with different emphasis on the impact depending on the target application.

In novel devices such as Quantum Dot (QD) solar cells and Intermediate Band (IB) solar cells, light-trapping has the potential to significantly increase the generally weak QD interband and intraband photo-generation. This may lead to the achievement of high efficiency QD solar cells operating in the thermally limited regime [4], and is a promising tool for the realization of IB solar cells [5].

In this work, we study light-trapping solutions for thin-film GaAs QD solar cells exploiting backside diffraction grating and conformal metal reflector. In such a scheme, the grating is designed to excite high order diffraction modes, which undergo total reflection at the cell top surface. Thus, the optical path length through the photoactive region and the carrier photo-generation are enhanced. In a previous work, we investigated diffraction gratings imprinted on the wide bandgap back surface field layer [6]. One potential issue with texturing the semiconductor surface is the possible increase of electrical parasitic loss due to the large interface area between the patterned semiconductor and the metal. In this work, we analyse the use of low-index and highly transparent dielectric gratings. Deposition of the dielectric materials and patterning of the photonic structures is carried out after wafer removal by techniques such as epitaxial lift-off [7] or substrate etching [8]. The dielectric material passivates the semiconductor surface, solving the concern of increased electrical loss. Moreover, such gratings can be fabricated with off-the-shelf dielectric materials routinely used in photolithography, allowing for easier experimental testing, and later translated into low-cost large-area manufacturing processes such as nano-imprint lithography [9].

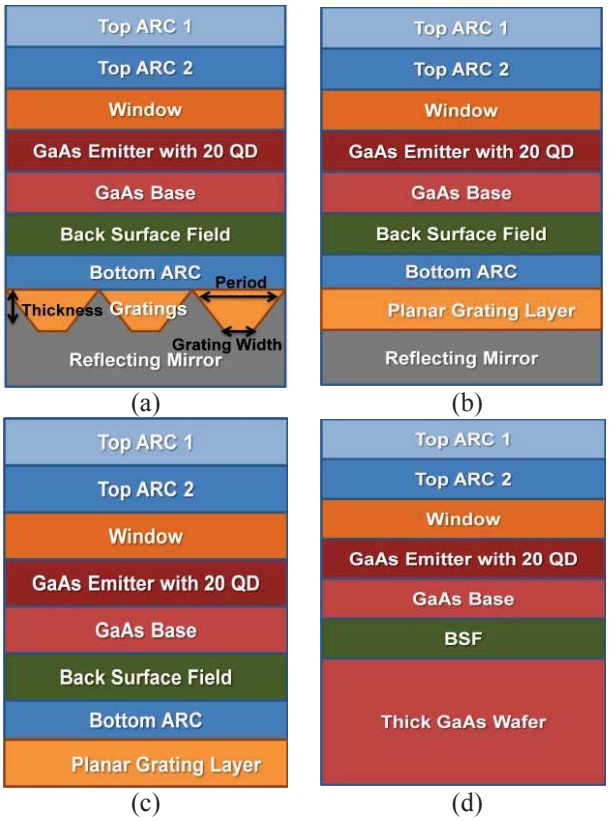

Fig.1 Studied solar cell configurations: (a) cell with grating layer and mirror; (b) planar cell with mirror; (c) planar cell without mirror; (d) cell on wafer.

2. Solar Cell Structures and Analysis Method

The thin-film solar cell structure in Fig. 1(a) includes a double-layer anti-reflection coating (SiN_x), window and back surface field layers realized by wide bandgap alloys, and a 2.6μm thick GaAs active region (base and emitter). A stack of 20 InAs/GaAs Quantum Dot layers, with overall thickness of about 400 nm, is embedded in the emitter next to the junction. The back grating, made with a low refractive index ($n \sim 1.5$) dielectric material, has a trapezoidal structure with linear tapering. Given the high mismatch between the refractive index of the semiconductor materials and the dielectric grating, an antireflection coating is interposed between the

back surface field and the grating layer in order to maximize the light coupling from the photoactive region to the diffraction grating. A conformal silver (Ag) mirror terminates the dielectric grating to maximize the rear side reflectivity. The performance of the solar cell with the rear grating in Fig. 1(a) is evaluated with respect to three reference structures: (b) a planar thin-film cell with Ag mirror; (c) a planar thin-film cell without Ag mirror; (d) a wafer-based cell. Both uni-periodic (1D) and bi-periodic (2D) gratings are used to examine the photocurrent enhancement.

In the planar configuration, the high reflectivity mirror allows to double the optical path length in the weak absorption regime. Higher enhancement of the optical path length of weakly absorbed photons and thus of photo-generation is achievable by using the textured grating with period larger than the incoming light wavelength. The grating is designed to couple a large fraction of the incoming light into high order diffraction modes propagating at angles larger than the cell escape cone (~16^o for a refractive index of 3.6), thus allowing for multiple internal reflections in the photoactive region.

The structures are simulated through the Synopsys RSoft tool diffractMOD [9], which implements the Rigorous Coupled Wave Analysis (RCWA) method. Material optical properties, included a realistic model of Ag, are taken from the literature [11] or from experimental characterization [9]. Taking advantage of the spectral separation of the QD and GaAs absorption, the QD layers are modelled as an effective medium whose absorption coefficient results from the linear superposition of the GaAs optical absorption and of the effective optical absorption of the nanostructured material (taking into account QD volume filling factor and QD size) [15].The effective optical absorption of the QD material is taken from typical literature data [12] derived from photoluminescence and external quantum efficiency spectra. The real part of the refractive index of the QD layers is then derived through Kramers-Kronig relation. The adopted detailed spectral dependence of the QD refractive index is reported in [6].

In order to single out the *useful* increase of optical absorption in the photoactive region from the optical loss in the electrically passive layers such as the ARC, grating and metal reflector, the absorbed photon density is computed region by region from the spatial distribution of the electromagnetic field. An example of calculated electrical field map under TE excitation, at wavelength of 1000 nm, is shown in Fig. 2 for the different structures under study. The standing wave patterns highlight the typical pattern of normal propagation in the planar cells (Fig. 2 (a) and (b)) and of propagating oblique modes in the cell with the diffraction grating (Fig. 2 (c)). Integration of the absorbed photon flux over the photoactive regions gives the fraction of *useful* absorbed photons per each wavelength (absorbance hereinafter) which, assuming a unitary internal quantum yield, provides the wavelength-dependent carrier photo-generation rate in the cell. As figure of merit for comparing the different structures, we consider the corresponding short circuit current density (J_{sc}), calculated by integrating over the wavelength range of interest the absorbance weighted by the incident solar spectrum. The estimation of J_{sc} is done on the basis of optical considerations only. However, in the devices under study, light trapping mainly acts on the longer wavelength range, where carrier collection efficiency can be made almost ideal by careful electrical design [13]-[15].

Normal incidence and terrestrial spectrum AM1.5G are assumed in the following.

4. Results

All the samples use the same two-layer ARC: the reflectance of the planar configuration without mirror is shown in Fig. 3. The optimization of the grating takes into account period, thickness, and the grating shape (from unpatterned planar structure – period=width – to triangular grating – width=0) with the target of maximizing the absorbed photon density in the photoactive regions. Regardless of the detailed grating shape, the aspect ratio (thickness/period) is revealed to be the most important design parameter. Moreover, the comparative analysis of the optimized gratings with different shapes points out that the optimal shape is the triangular one.

Fig. 4 shows the dependence of the attainable J_{sc} in the triangular grating configuration, as a function of the aspect ratio, for different grating periods. The analysis takes into account TE polarization only, as it provides the largest power coupling to diffraction modes in the absorbing region. On the other hand, TM polarization is dominated by optical loss induced by surface plasmons at the grating-mirror interface and marginally contributes to the useful absorption enhancement.

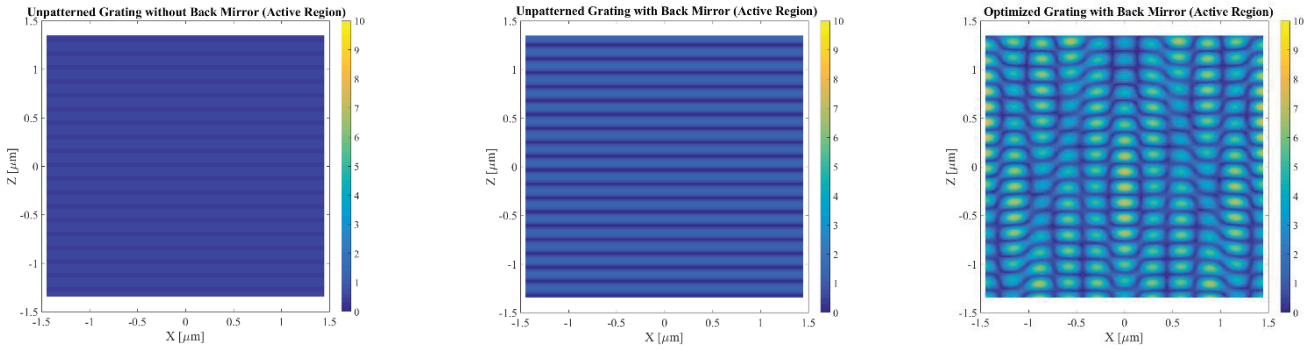

(a) (b) (c)

Fig. 2 Map of the calculated electrical field amplitude (TE excitation) at λ = 1000 nm in the 2.6 μm GaAs-QD photoactive region for the different configurations under study: (a) planar cell without mirror; (b) planar cell with mirror; (c) cell with rear side triangular grating (3μm period and 750 nm height) and mirror.

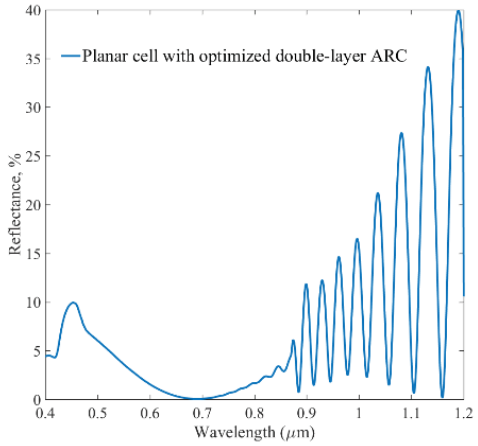

Fig. 3 Reflectance of the planar cell with optimized double-layer ARC.

Optimum aspect ratio ranges between 0.2-0.4 for grating periods ranging from 1.5 µm to about 4 µm. The maximum variation of J_{sc} with respect to the optimum value when the period changes from 1.5 µm to 3 µm period is less than 5%; thus a period of 3 µm is selected for further analysis, due to the easier fabrication. For the selected configuration (period=3 µm, height=0.75 µm), Fig. 5 analyses the impact of the detailed shape of the grating on the achievable J_{sc}. The optimum shape results to be the triangular one (grating width=0). In fact, the triangular shape diffracts a higher fraction of the incoming light, and thus provides enhanced light-trapping and higher J_{sc}. Moving to bi-periodic gratings, higher efficiency enhancement is expected for pyramidal gratings with respect to more rounded geometries [16].
Finally, the absorbance spectrum computed from the integration of the photon flux in the active region is reported in Fig. 6 for the different configurations. The absorbance of the wafer-based cell (not shown) is almost coincident with that of the planar cell without mirror. The optimized pyramidal grating shows a significant increase of absorption in the QD wavelength region with respect to the reference planar structures. The corresponding short circuit current densities under AM1.5G illumination are summarized in

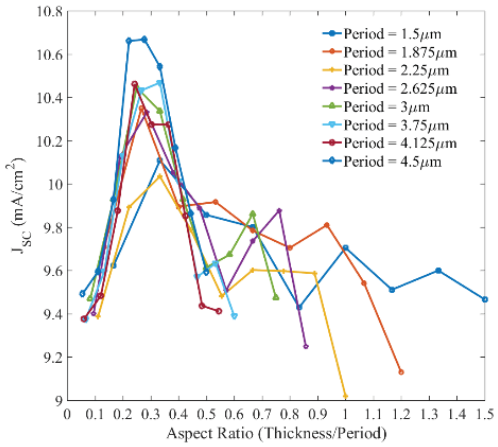

Fig. 4 Dependence of J_{sc} (0.75 µm - 1.2 µm wavelength range, TE polarization) as a function of the aspect ratio for different periods for the triangular grating configuration.

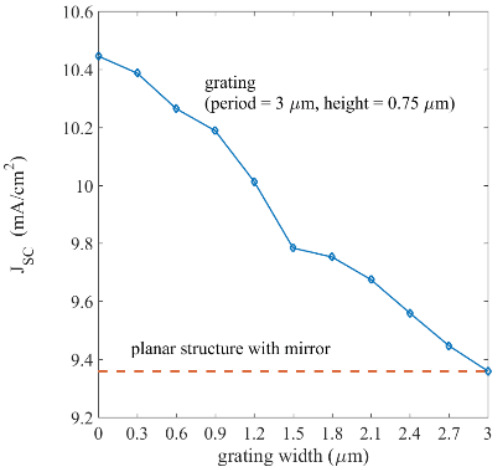

Fig. 5 Dependence of J_{sc} (0.75 µm - 1.2 µm wavelength range, TE polarization) as a function of the uni-periodic grating width: width=0 indicates the triangular grating, width=3 µm identifies the unpatterned planar structure.

Table 1, for the wavelength ranges of 0.75 µm - 1.2 µm (GaAs band-edge and QD) and 0.895 µm - 1.2µm (QD only). Owing to the enhancement of the attainable current in the cell with optimized textured grating with respect to the unpatterned cell, the 20 QD layer stack provides the same current as a stack with about 50 and 80 QD layers for the 1D and 2D gratings, respectively, with the obvious advantage of simplifying the epitaxial growth and limiting strain issues. Moreover, even assuming ideal QD epilayers without any degradation of the crystal material quality, the unavoidable penalty in the open circuit voltage induced by the QD layers remains limited.

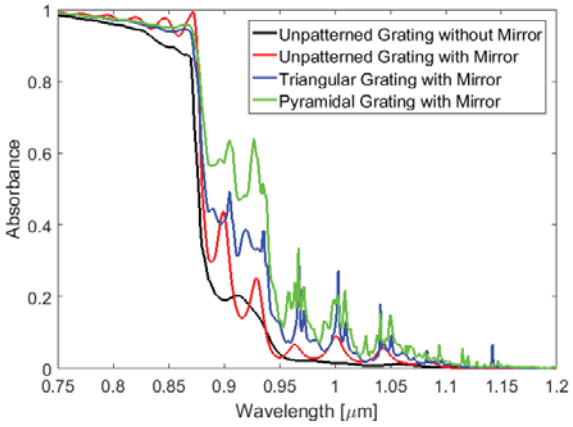

Fig. 6 Spectral dependence of the active region absorbance in planar cell without mirror, planar cell with mirror, cell with triangular grating (period=3 µm, thickness=0.75 µm) and mirror, and cell with pyramidal grating (period=3 µm, thickness=0.75 µm) and mirror. Average TE and TM polarization.

5. Conclusion

Light trapping is a viable tool to solve the issue of low absorption of sub-bandgap quantum dot states, and enable

high efficiency quantum dot solar cells and intermediate band solar cells.

A light-trapping design for quantum dot solar cells in thin-film configuration is examined, based on the use of rear side diffraction gratings and conformal silver mirror. The analysed uni-periodic and bi-periodic gratings are patterned on dielectric materials that also act as passivating layers for the semiconductor surface. Photonic design optimization is carried out through full-wave electromagnetic simulations based on rigorous coupled wave analysis. The predicted enhancement of quantum dot photo-generation allows up to quadrupled current density from the quantum dot stack. This relaxes the need of complex strain balanced epitaxial growth to increase the number of quantum dot layers and keeps low the inherent open circuit voltage penalty induced by the quantum dot layers. Due to the ease of fabrication, the proposed structures provide a useful platform for the development and assessment of photonic management in thin-film QD cells.

Table 1: Short circuit current and gain in the different structures at AM1.5G. The maximum J_{sc} that can be converted from the incident spectrum is 22.52 mA/cm^2 and 12.99 mA/cm^2 in the ranges 0.75-1.2 μm and 0.895-1.2 μm, respectively.

Structure	Unpatterned cell without Mirror	Unpatterned cell with Mirror	Triangular Grating with Mirror (TE/TM Avg.)	Pyramidal Grating with Mirror
J_{SC} (0.75μm to 1.2μm) [mA/cm^2]	8.5800	9.3594	9.8891	10.7307
Enhancement (0.75μm to 1.2μm)	-	1.0908	1.1526	1.2507
J_{SC} (0.895μm to 1.2μm) [mA/cm^2]	0.4831	0.7609	1.2643	1.8995
Enhancement (0.895μm to 1.2μm)	-	1.5750	2.6170	3.9319

Acknowledgements

The research was supported by the European Union's Horizon 2020 research and innovation program, under Grant Agreement 687253 – TFQD. http://tfqd.eu

References

[1] Lush, G., and Lundstrom, M., "Thin film approaches for high-efficiency III–V cells." Solar cells 30.1-4 (1991): 337-344.

[2] Mokkapati, S. and Catchpole, K. R., "Nanophotonic light trapping in solar cells", *J. Appl. Phys*., 112, 101101 (2012).

[3] Brongersma, Mark L., Cui, Yi, Fan, Shanhui, "Light management for photovoltaics using high-index nanostructures", Nat. Mater., Vol. 13, no. 5, pp. 451-460, 2014.

[4] Cappelluti, F., Gioannini, M., Ghione, G., et al., "Numerical Study of Thin-Film Quantum-Dot Solar Cells Combining Selective Doping and Light-Trapping Approaches," 43rd IEEE PVSC, Portland, Oregon, (2016).

[5] Mellor, A., Luque, A., Tobías, I., and Martí, A., "The feasibility of high-efficiency InAs/GaAs quantum dot intermediate band solar cells," *Solar Energy Materials and Solar Cells*, *130*, pp.225-233.

[6] Musu, A., Cappelluti, F., Aho, T., et al., "Nanostructures for light management in thin-film GaAs quantum dot solar cells," In Solid-State Lighting (pp. JW4A-45), 2016, November. Optical Society of America.

[7] Bauhuis, G.J., Mulder, P., Haverkamp, E.J., et al., "26.1% thin-film GaAs solar cells using epitaxial lift-off ", Sol. Energy Mat. Sol. Cells, 93, 1488 (2009).

[8] Lee, S.M., Kwong, A., Jung, D., et al., "High performance ultrathin GaAs solar cells enabled with heterogeneously integrated dielectric periodic nanostructures", *ACS Nano*, 9(10), pp.10356-10365.

[9] Tommila, J., Polojärvi, V., Aho, A., et al., "Nanostructured broadband antireflection coatings on AlInP fabricated by nanoimprint lithography," *Solar Energy Materials & Solar Cells*, 94 (10), pp. 1845-1848 (2010).

[10] https://optics.synopsys.com/rsoft/rsoft-passive-device-diffractMOD.html, accessed May 2017.

[11] Palik, E.D., 1998. *Handbook of optical constants of solids* (Vol. 3). Academic press.

[12] Cappelluti, F., Gioannini, M., Khalili, A., "Impact of doping on InAs/GaAs quantum-dot solar cells: A numerical study on photovoltaic and photoluminescence behavior," *Solar Energy Materials and Solar Cells*, 157 (2016): 209-220.

[13] Walker, A.W., Höhn, O., Micha, D.N., et al., "Impact of photon recycling on GaAs solar cell designs," *IEEE Journal of photovoltaics*, *5*(6), pp.1636-1645.

[14] Bauhuis, G., Mulder, P., Hu, Y.Y., et al., "Deep junction III–V solar cells with enhanced performance," *physica status solidi (a)*, 2016.

[15] Gioannini, M., Cedola, A., Di Santo, N., et al., "Simulation of quantum dot solar cells including carrier intersubband dynamics and transport," *IEEE J. Photovoltaics*, vol. 3, no. 4, pp. 1271–1278, Oct 2013.

[16] Zhang, A., Guo, Z., Tao, Y., et al., "Advanced light-trapping effect of thin-film solar cell with dual photonic crystals," *Nanoscale Res. Lett.*, 10(1), p.214 (2015).

[17] Chong, Teck Kong, et al. "Optimal wavelength scale diffraction gratings for light trapping in solar cells." Journal of Optics 14.2 (2012): 024012.